



Pergamon

Tetrahedron 56 (2000) 1637–1647

TETRAHEDRON

An Ab initio Molecular Orbital Study on the Magnesium Controlled 1,3-Cycloaddition of Nitrile Oxides and Allylic Alcohols with Regio- and Stereoselectivity

Shohei Fukuda,^{a,b} Akio Kamimura,^a Shuji Kanemasa^c and Kenzi Hori^{a,*}^aDepartment of Applied Chemistry and Chemical Engineering, Yamaguchi University, Tokiwadai, Ube 755-8611, Japan^bAgrochemical Research Department, Ube Laboratory, Ube Industries, Ltd., 1978-5 Kogushi, Ube 755-8633, Japan^cInstitute of Advanced Material Study, Kyushu University, Kasugakoen, Kasuga 816-8580, Japan

Received 30 September 1999; accepted 13 January 2000

Abstract—Ab initio molecular orbital calculations at the MP4(SDTQ)/6-31G^{*}/RHF/6-31G^{*} level of theory were used to obtain detailed insight into the reaction profile on the Mg controlled 1,3-cycloaddition of nitriles oxide with allylic alcohols. It was confirmed that the complex formation reduces the HOMO–LUMO energy gaps of the two reactants. The propensity correlates well to calculated activation energies of the cycloaddition. The *syn*-stereoselectivity depends on the steric repulsion between the vinyl fragment and the substituent at the α -position of the alcohol or alkoxide. THF or Et₂O in the reaction mixture prevent the coordination of R¹CNO from forming the Mg intermediate and result in decelerating the cycloaddition. The results obtained in the present study well explain an important role of the Mg²⁺ ion in the 1,3-dipolar cycloadditions of nitrile oxides with allylic alcohols. © 2000 Elsevier Science Ltd. All rights reserved.

Introduction

The nitrile oxide cycloaddition (NOC) reaction is one of the most useful methods in organic synthesis.¹ The reaction proceeds via a concerted process like Diels–Alder reaction does. The regio- and stereochemical control of the reaction has been of interest so far and many efforts have been reported.² In contrast with the Diels–Alder reaction, however, it is not always easy to accomplish good regio- and/or stereoselectivity for the reaction. The reaction of benzonitrile oxide with crotonate ester, for example, gave possible two regioisomers in the ratio of 66:34^{3,4} although there are a few examples of regioselective NOC reactions.⁵ In order to explain these experimental results, Houk and his coworkers proposed the inside alkoxy effect that the ether moiety in allylic ether prefers the inside position at the RHF/3-21G level of theory.⁶ They also pointed out that the OH group of allylic alcohol prefers the outside position due to formation of a hydrogen bond with the oxygen atom in nitrile oxide.

The most difficult drawback to control the reactions is that use of Lewis acid, which gave many successful examples in the Diels–Alder reactions, usually deactivates nitrile oxides and the reaction itself stops. Recently, a good methodology

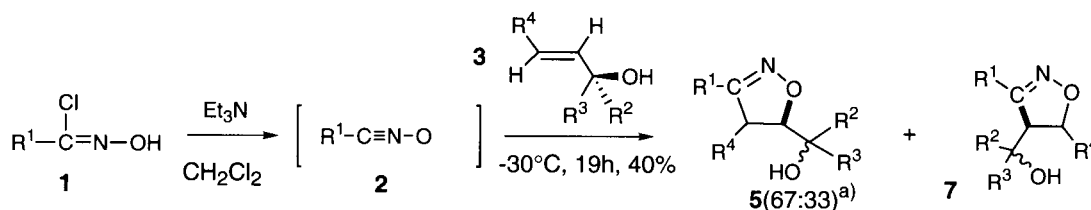
to overcome the status has been reported, in which the NOC reaction in the presence of magnesium ion is accelerated as well as controlled regio- and stereoselectively to give single isomer of 2-isoxazolines in good yields.⁷ Preliminary results of ab initio molecular orbital (MO) calculations explained why the Mg ion control-technique works well for the selectivity. However, we realized these simple geometry optimizations at the RHF/3-21G^{*} level of theory was not enough to understand whole reaction profile of the NOC reaction. This prompted us to extend our theoretical investigations including transition state (TS) geometries as well as energy relations at the MP4(SDTQ)/6-31G^{*}/RHF/6-31G^{*} level of theory. In the present study, we provided a detailed analysis of the Mg²⁺ ion coordination-control in the NOC reactions using ab initio MO calculations.

The Mg complexes coordinating a nitrile oxide and an allylic alcohol are considered to be key intermediates for the regio- and stereoselective NOC reactions. We examined various reaction conditions such as reaction temperature, reaction time, amount of bases, kind of solvents and the addition order of reagents in order to improve yields and selectivities of the reaction.^{7b} Those were classified into three types of reactions. The first, Type I reaction in Scheme 1, is that between allylic alcohol and nitrile oxide in absence of Mg²⁺ ion. This reaction uses Et₃N as base for generating R¹CNO **2** from benzohydroximinoyl chloride **1**.

In Type II reaction (Scheme 2), EtMgBr first reacts with **1** to form **2**, followed by generation of **9**, and then, allylic

Keywords: nitrile oxide; cycloaddition; theoretical studies; transition state; regio control; stereo control.

* Corresponding author. Tel.: +81-836-35-9045; fax: +81-836-35-9933; e-mail: kenji@sparklx.chem.yamaguchi-u.ac.jp



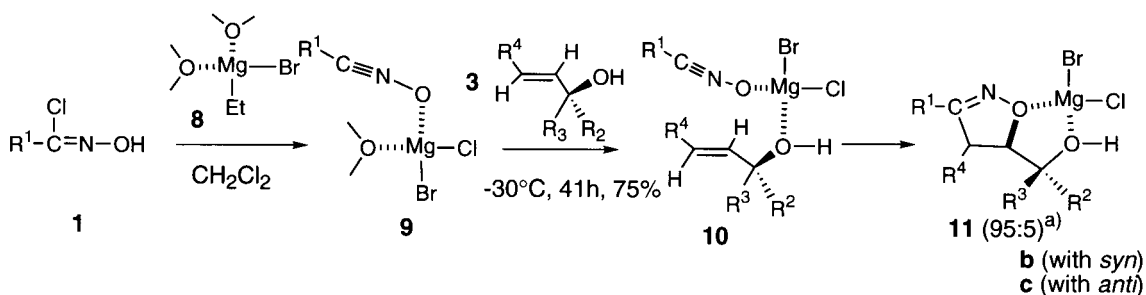
Scheme 1. Type I: Hydroximinoyl chloride **1** and allylic alcohol **3** were treated with Et_3N ; *syn/anti* ratio in product.

alcohol was added. In the reaction, EtMgBr has two roles; one is the role as a base to generate **2** from **1**; the other is that as a central metal which is effective to gather the two reactants, nitrile oxide and allylic alcohol, in the complex. In Type III reaction (Scheme 3), allylic alkoxide instead of the alcohol in Type II reaction is a ligand in the Mg^{2+} complex. Allylic alcohol **3** was first treated with EtMgBr to produce an Mg^{2+} complex **12** having an alkoxide and two THF ligands. Then **12** reacts with **2** to form a reactant complex **13**.

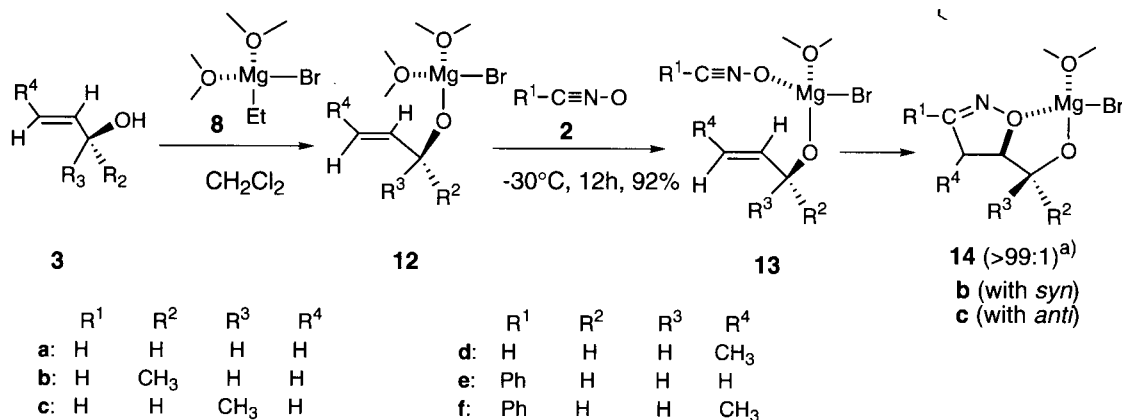
In order to analyze these detailed experimental results, we performed ab initio MO calculations, which simulate the methods adopted in our experiments. Stable and transition state (TS) geometries were optimized for model reactants of Mg^{2+} complexes, and then, the activation energies for each mechanism were estimated. It was confirmed that these calculated results were very effective to analyze the NOC in detail.

Method of Calculation

Ab initio MO calculations were performed by using the Gaussian94 program.⁸ All the geometries were fully optimized at the RHF/6-31G* level of theory and checked by looking through vibrational frequencies. Frontier Orbital analysis at the RHF/6-31G* MOs was carried out with the WinMOPAC Version 2 program⁹ by displaying shapes of the highest occupied MOs (HOMOs) and the lowest unoccupied MOs (LUMOs) and by checking their orbital energies. Intrinsic reaction coordinates (IRCs)¹⁰ were also calculated to analyze the mechanism in detail for all the TSs obtained. Since the order of activation energies at the MP2/6-31G**/RHF/6-31G* level of theory were not consistent with the experimental results, the MP4(SDTQ)/6-31G* calculations were performed to refine energy relation among reactants, TSs and products. It is necessary to note



Scheme 2. Type II: **1** was treated with EtMgBr (1 M solution in THF), then **3** was added; *syn/anti* ratio in product.



Scheme 3. Type III: **3** was treated with 2 equiv. mol EtMgBr (1 M solution in THF), then **1** was added. (a) *syn/anti* ratio in product.

that the RHF calculations overestimated the activation energies of the NOC reactions more than 20 kcal mol⁻¹. Solvent effect for the NOC reaction was estimated by calculating SCRF energies for the optimized geometries at the RHF/6-31G* level of theory. The activation energies including the effect listed in Table 1 are not much different from in vacuum ($\sim\pm 2.0$ kcal mol⁻¹). Therefore, we have used the MP4(SDTQ) energies for discussion unless otherwise noted.

In the present study, HCNO is the model of **2** and Br in the complexes is replaced to Cl, butanol to methanol, THF to dimethyl ether to simplify the calculations. Table 1 summarizes total energies and activation energies of the reactions. Table 2 lists the optimized parameters of geometries for the reactants and TSs.

Results and Discussion

Frontier molecular orbital analysis in the Mg complexes

The frontier orbital theory has been used for explaining regioselectivity of the NOC reactions¹¹ which are governed by the interaction between HOMO of dipole (π_{CNO}) and LUMO of dipolarophile ($\pi_{\text{C}=\text{C}}^*$) or that between LUMO of dipole (π_{CNO}^*) and HOMO of dipolarophile ($\pi_{\text{C}=\text{C}}$). We call the former HO control interaction and the later LU control interaction in present study according to Sustman's classification.¹² MO coefficients and orbital energies in the two reactants, HCNO and allylic alcohol, determine the reactivity of the reaction. It is very difficult to analyze the coefficients for regioselectivity in detail because we used split valence basis sets (6-31G*) for the ab initio MO calculations. As will be discussed later, the Mg²⁺ coordination of the two ligands is responsible for the high regioselectivity of the reaction. Therefore, only the reactivity of the reactants was discussed on the basis of the HOMO–LUMO energy gaps in the model complexes.

In the Mg²⁺ complexes, it is possible to find their HOMOs localized around the dipolarophile and LUMOs around dipoles as shown Fig. 1.¹³ These orbitals relate to the LU control interaction. Table 3 summarizes orbital energies of these MOs together with those for the HO control interaction. As π_{CNO}^* interacts with $\pi_{\text{C}=\text{C}}$ even in the complexes, we can make discussions of the reactivity similar to that in previous papers.⁷ As the orbital energies of $\pi_{\text{C}=\text{C}}$ in **3a** and π_{CNO}^* in **2a** turned out to be -0.371 and 0.195 Hartree, the HOMO–LUMO energy gap for the LU control (LU gap) is 0.566 Hartree for the free reactants. As the energy gaps between the MOs in **4a**, a precursor leading to **5a**, is 0.544 Hartree which is smaller by 0.022 Hartree than that of the free reactants. On the other hand, the energy gaps for the HO control orbitals (HO gap) is 0.588 Hartree which is larger by 0.044 than LU gap. Moreover, the LU gaps in the Mg complexes are small more than 0.1 Hartree in comparison with the HO gaps. It is, therefore, considered that the NOC reactions of the reactant Mg complexes are governed by the LU control interaction.

The coordination of two ligands to Mg²⁺ decreases the LU gap only by 0.009 Hartree in **10a**, the reactant of Type II

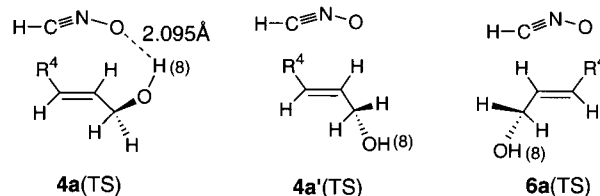
reaction, in comparison with that in **4a**. The ligand exchange of allylic alcohol to allylic alkoxide produces another 0.046 Hartree decrease in the LU gap for **13a**, the reactant of Type III reaction. As interaction with smaller MO gap results in higher reactivity, Type III reaction with an alkoxide ligand is the most reactive. It is important to point out that the coordination of the two reactants reduces the LU gap between frontier MOs, i.e. the coordination enhances the reactivity of the NOC reactions as observed.^{7b}

Non-magnesium reaction (Type I reaction)

The regioselectivity is almost achieved for the NOC reactions with mono substituted alkenes without using Mg²⁺ although it is possible to consider two types of products, 4- and 5-substituted-isooxazoline, **5** and **7** shown in Scheme 1. For example, **5** was predominately yielded as the product of the reaction with benzonitrile oxide and 1-buten-3-ol.^{7b} On the other hand, the regiochemical control was poor for reactions of α,β -disubstituted alkenes except for a few successful examples.⁵ Houk et al. pointed out that hydrogen bond plays an important role in achieving this selectivity.⁶ Like the Mg²⁺ complexes, the weak bond also makes it possible to locate the oxygen atom of allylic alcohol at the outside position in Houk's TS model. Therefore, it is very useful to investigate the non-magnesium NOC reactions in order to understand the Mg effect in detail.

There are no large differences in TS geometries around the isooxazoline five-membered rings, which have not formed yet in **4(TS)** and **6(TS)** in Fig. 2. A remarkable difference between these TS geometries is whether or not a hydrogen bond exists; O(1) of HCNO in **4e(TS)** makes a hydrogen bond with H(8) of allylic alcohol since the distance between these atoms was calculated to be 2.078 Å. On the other hand, there is no such bond in **6e(TS)** in which the H(8) locates far away from O(1). This feature in geometry stabilizes **4e(TS)** by 4.9 kcal mol⁻¹ in comparison with **6e(TS)** at the MP4(SDTQ)/6-31G*//RHF/6-31G* level of theory. The energy difference between **4a(TS)** and **6a(TS)** turned out to be 4.9 kcal mol⁻¹. The large Ph substituent in the nitrile oxide does not change the energy difference relating to the regioselectivity at all. According to energy differences between **4(TS)** and **6(TS)** in Table 4, **4(TS)** is more stable than the corresponding **6(TS)**.

The change in geometry from **4a(TS)** to **4a'(TS)** results in loss of the hydrogen bond so that **4a'(TS)** is less stable by 3.9 kcal mol⁻¹ than **4a(TS)**. The geometry without the weak bond is almost as unstable as **6a(TS)**. It is considered that the O(1)–H(8) hydrogen bond is effective for the regioselectivity. Curran discussed the regioselectivity based on the hydrogen bond from their experimental data.^{5g}



In order to estimate steric effect for regioselectivity, we also

Table 1. Total energies (Hartree) for the reactants, TSs and products and activation energies

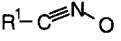
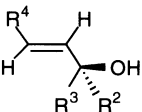
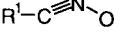
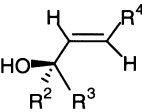
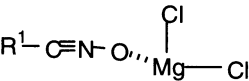
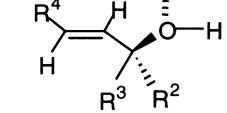
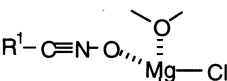
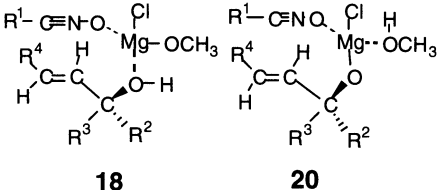
Reaction Type	Compound	RHF/6-31G [*] //RHF/6-31G [*]	ΔE^a kcal mol ⁻¹	MP4/6-31G [*] //RHF/6-31G [*]	ΔE^a kcal mol ⁻¹
HCNO	2a	-167.63043		-168.13766	
CH ₂ =CHCH ₂ OH	3a	-191.91503		-192.52771	
MgCl ₂		-1118.72715		-1119.04012	
Type I					
	2a + 3a	-359.54546	8.4 ^b	-360.66537	9.1 ^b
	4a	-359.55890	0.0	-360.67988	0.0
	4a(TS)	-359.50241	35.4 ^b (32.1)	-360.65893	13.1 ^b
	4a'(TS)	-359.4946310	40.3 ^b (38.4)	-360.6527662	17.0 ^b
	5a	-359.63150	-45.6 ^b	-360.74227	-39.1 ^b
4(TS)					
	6a(TS)	-359.49015	43.1 ^b (41.0)	-360.65112	18.0 ^b
	7a	-359.63090	-45.2 ^b	-360.74294	-39.6 ^b
	4d(TS)	-398.53644		-399.84322	
	4e(TS)	-589.06188		-591.04008	
	4f(TS)	-628.09522		-630.22644	
	6d(TS)	-398.53005		-399.83809	
	6e(TS)	-589.04938		-591.03222	
	6f(TS)	-628.08909		-630.22026	
6(TS)					
Type II					
	2a + 3a + MgCl₂	-1478.27261	53.1	-1479.70549	51.9
	10a	-1478.35720	0.0	-1479.78817	0.0
	10a(TS)	-1478.29961	36.1 (34.5)	-1479.76636	13.7
	11a	-1478.42410	-42.0	-1479.85547	-42.2
	10b	-1517.39747	0.0		
	10b(TS)	-1517.33965	36.3		
	11b	-1517.46511	-42.4		
	10c	-1517.39364	2.4 ^c		
	10c(TS)	-1517.33634	38.4 ^c		
	11c	-1517.46277	-41.0 ^c		
10					
Type III					
	13a	-1172.31669	0.0	-1174.09016	0.0
	13a(TS)	-1172.27062	28.9 (30.2)	-1174.07018	12.5
	14a	-1172.39428	-48.7	-1174.16711	-48.3
	13b	-1211.35686	0		
	13b(TS)	-1211.31069	29.0		
	14b	-1211.43516	-49.1		
	13c	-1211.35459	1.4 ^d		
	13c(TS)	-1211.30844	30.4 ^d		
	14c	-1211.43162	-46.9 ^d		
13					

Table 1 (continued)

Reaction Type	Compound	RHF/6-31G [*] //RHF/6-31G [*]	ΔE^a kcal mol ⁻¹	MP4/6-31G [*] //RHF/6-31G [*]	ΔE^a kcal mol ⁻¹
Proton exchange type					
	16a	-1119.72405	0.0	-1121.33824	0
	16H(TS)	-1119.70644	11.1 ^c	-1121.33013	5.1 ^c
	17a	-1119.72589	-1.2 ^c	-1121.33996	-1.1 ^c
	18H(TS)	-1133.27078	10.4	-1134.90680	4.7
	18a	-1133.28736	0.0	-1134.91427	0.0
	18a(TS)	-1133.22767	37.5 ^f (44.3)	-1134.88911	15.8 ^f
	19a	-1133.35391	-41.8 ^f	-1134.97850	-40.3 ^f
	20a	-1133.28955	-1.4 ^f	-1134.91629	-1.3 ^f
	20a(TS)	-1133.24314	27.7 ^f (31.4)	-1134.89573	11.6 ^f
	21a	-1133.36687	-49.9 ^f	-1134.99280	-49.3 ^f

^a Activation energy from reactant. The values in parentheses are the activation energies estimated by SCRF-IPCM method at RHF/631-G^{*} level of theory.

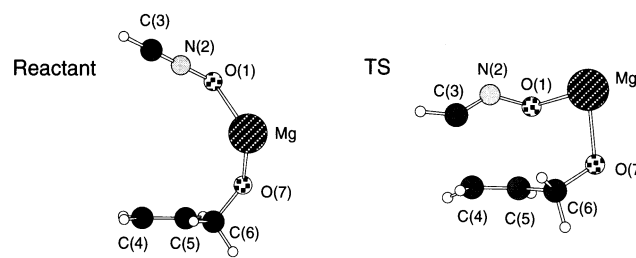
^b Energy relative to that of **6a**.

^c Energy relative to that of **10b**.

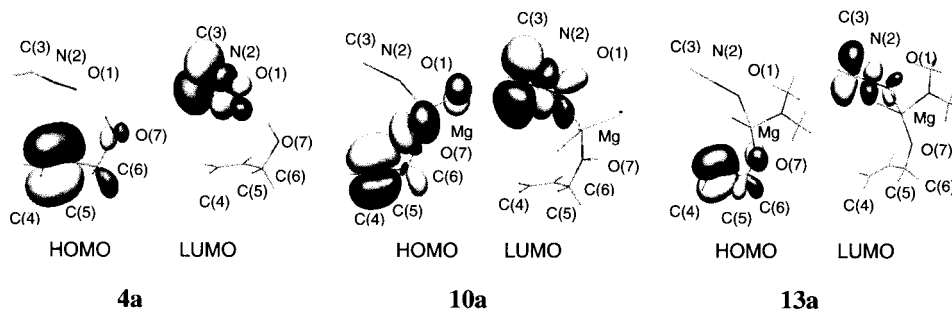
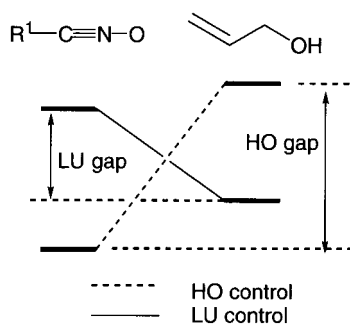
^d Energy relative to that of **13b**.

^e Energy relative to that of **16a**.

^f Energy relative to that of **18a**.

Table 2. Optimized bond lengths (Å), Bond Angles (°) for the reactants and TSs for NOC reactions


	Type I		Type II		Type III		Type II		Type III	
	4a	4a(TS)	10a	10a(TS)	13a	13a(TS)	18a	18a(TS)	20a	20a(TS)
$\Delta E(\text{kcal mol}^{-1})$	–	13.1	–	13.7	–	12.5	–	15.8	–	12.9
Mg–O(1)	–	–	2.082	2.034	2.115	2.035	2.088	2.056	2.100	2.025
Mg–O(7)	–	–	2.051	2.124	1.837	1.886	2.078	2.137	1.830	1.881
O(1)–C(5)	3.576	2.286	4.574	2.402	3.967	2.710	4.658	2.393	3.953	2.716
C(3)–C(4)	3.660	2.156	5.805	2.103	5.264	2.119	5.718	2.104	5.868	2.122
O(1)–Mg–O(7)	–	–	105.0	81.9	111.5	97.8	106.8	81.4	111.8	98.3

**Figure 1.** HOMOs and LUMOs for the LU control interaction in **4a**, **10a** and **13a**.**Table 3.** Orbital energies of and HOMO–LUMO energy gaps (Hartree) for reactants

Type	HO control			LU control			
	π_{CNO}	$\pi_{\text{C=C}}^*$	HO gap	$\pi_{\text{C=C}}$	π_{CNO}^*	LU gap	
2a+3a	I	-0.404	0.176	0.581	-0.371	0.195	0.566
4a	I	-0.418	0.170	0.588	-0.365	0.179	0.544
6a	I	-0.383	0.150	0.533	-0.393	0.215	0.608
10a	II	-0.478	0.169	0.647	-0.394	0.141	0.535
13a	III	-0.465	0.218	0.683	-0.336	0.142	0.478
18a	II	-0.472	0.184	0.656	-0.378	0.146	0.524
20a	III	-0.468	0.218	0.686	-0.335	0.143	0.478

optimized TS geometries with a methyl group at the γ -position such as **4d**(TS) and **6d**(TS) ($R^1=R^2=\text{Me}$), **4f**(TS) and **6f**(TS) ($R^1=\text{Me}$, $R^2=\text{Ph}$). The energy difference between **4d**(TS) and **6d**(TS) was calculated to be $3.2 \text{ kcal mol}^{-1}$. The methyl group as R^2 reduces the **4**(TS)–**6**(TS) energy difference by $1.7 \text{ kcal mol}^{-1}$. The decrease in this difference was not so large for nitrile oxide with a phenyl substituent; the **4f**(TS)–**6f**(TS) energy difference is $3.9 \text{ kcal mol}^{-1}$ whose value is smaller by $1.0 \text{ kcal mol}^{-1}$ than the corresponding value for **4e**. The remaining difference in energy corresponds to that originated from the hydrogen bond. This result is similar to that pointed out by Houk et al.¹⁴

It is considered that the calculated energy differences between **4**(TS) and **6**(TS) are large enough to accomplish the highly regioselective NOC reactions with crotonyl alcohols. However, a mixture of the possible two regioisomers were obtained in most of the NOC reactions performed in solvents with good hydrogen acceptor such as DMF and Et_2O in practice.^{5g,6} This is probably due to the solvent that weakens the hydrogen bonds in question. Even so, the present results show that the hydrogen bond must be useful to gather and place oxygen atoms of the reactants in NOC reactions. This feature in geometry is very important to

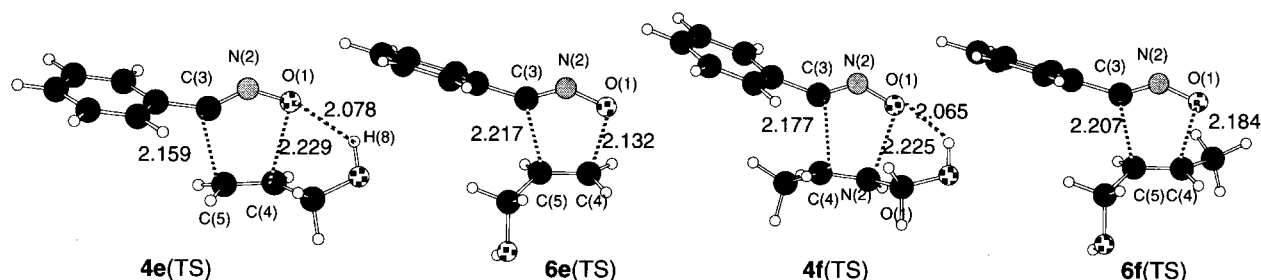


Figure 2. TS structures of 4e(TS), 6e(TS), 4f(TS) and 6f(TS).

Table 4. Energy differences (ΔE) between 4(TS) and 6(TS)

	R ¹	R ⁴	ΔE^a (kcal mol ⁻¹)
4a(TS)–6a(TS)	H	H	–4.9
4a(TS)–4a'(TS)	H	H	–3.9
4d(TS)–6d(TS)	H	CH ₃	–3.2
4e(TS)–6e(TS)	Ph	H	–4.9
4f(TS)–6f(TS)	Ph	CH ₃	–3.9

^a The values estimated from total energies in Table 1.

achieve the regioselectivity in products. If the stability of the geometry in the TS was enhanced by a similar effect, the NOC reactions would proceed regioselectively even though 1,2-substituted allylic alcohols are used. Thus, the following magnesium control technique is regarded as the best extension of the strategy.

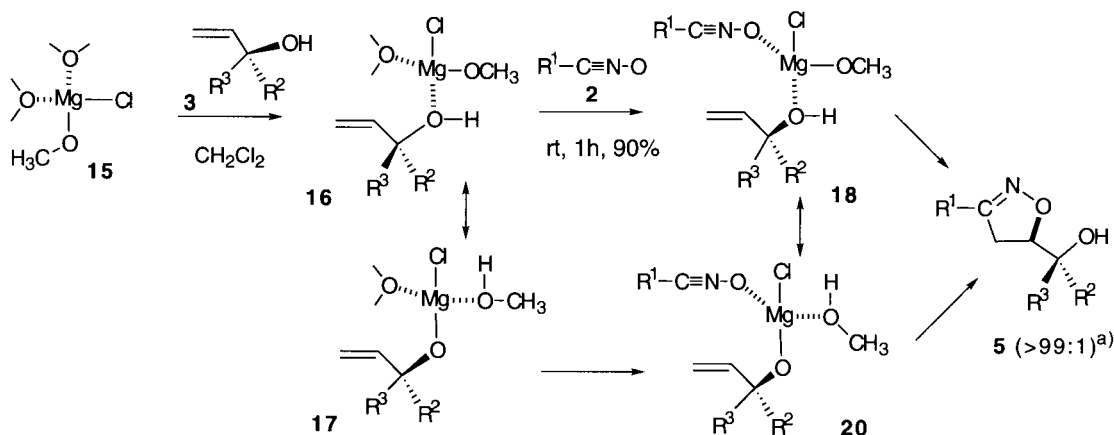
The NOC reactions in alcohol–Mg and alkoxide–Mg complexes (Type II and III reaction)

The NOC reaction proceeds through a Mg²⁺ complex **10a** which has the two oxygens of the alcohol and the nitrile oxide coordinating to the central metal in Type II reaction

of Scheme 2. Mg–O(1) and Mg–O(7) distances in **10a** were calculated to be 2.082 and 2.051 Å, respectively (Table 2). Although O(1)–C(5) and C(3)–C(4) distances (4.574 and 5.805 Å, respectively) are rather long even in the complex, Mg²⁺ of Lewis acid succeeds in gathering the reactants of the cycloaddition. This geometry is suitable for obtaining a regioselective product **11a**. The activation energy was calculated to be 13.7 kcal mol⁻¹. It was observed that benzonitrile oxide **2e** reacted with 1-penten-3-ol (**3**: R²=Et, R³, R⁴=H) to give corresponding **5** in 75% yield with complete regioselectivity.^{7b} However, 2-butene-1-ol (**3**: R², R³=H, R⁴=Me), which has a methyl group at the γ -position, reacts with **2e** to give the mixture of **5** and **7**. This reaction has no selectivity with the **5/7** ratio=55/45.

The simplest model for Type III reaction (Scheme 3) is **13a** which has a dimethyl ether instead of THF used in experiments. The Mg–O(7) distance was calculated to be 1.837 Å which is shorter by 0.214 Å than that of **10a**. The oxygen atom of the alkoxide binds to Mg²⁺ stronger than that in allylic alcohol. The activation energy turned out to be 12.5 kcal mol⁻¹ which is lower by 1.2 kcal mol⁻¹ than that of **10a**. Therefore, the alkoxide is more reactive than the alcohol. This result is consistent with that from HOMO–LUMO energy gaps as discussed above. It was observed that the **5/7** ratio in Type III reaction of **2e** and 2-buten-1-ol was more than 99:1 (Type III).^{7b} According to these results, alkoxides are ligands much more suitable for regioselectivity than alcohols.

There is a good experimental example⁷ to understand the difference of reactivity between Type II and III reactions



Scheme 4. (a) *syn/anti* ratio in product.

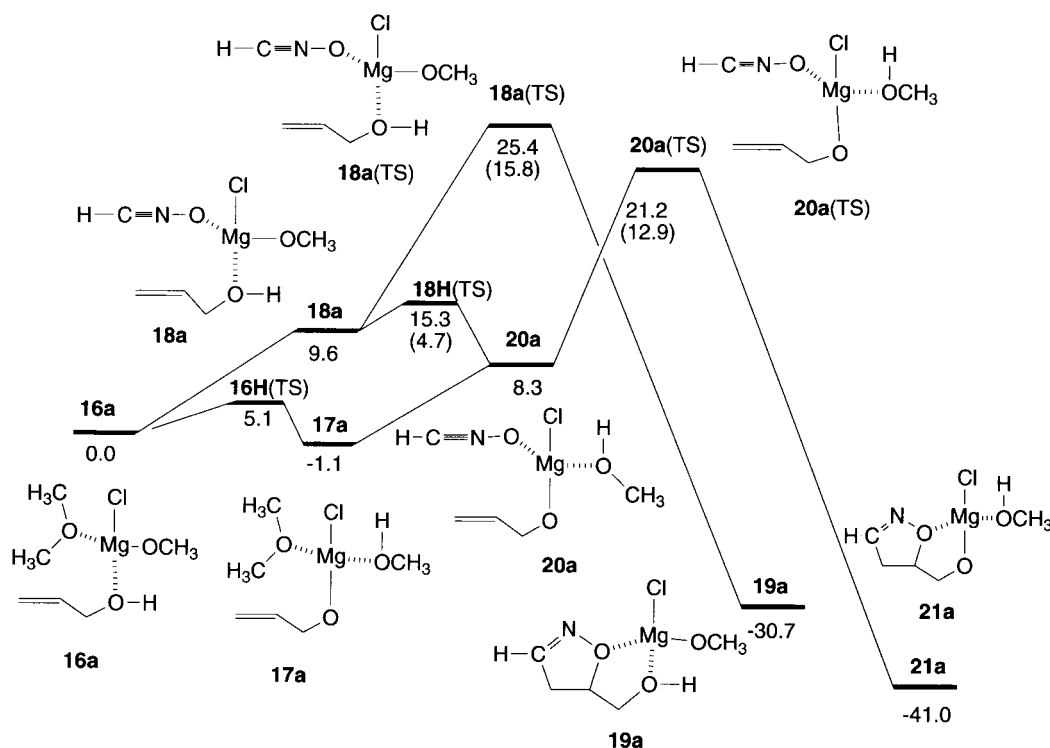


Figure 3. Energy-level diagram for Scheme 4. Values in parentheses are the activation energies for the corresponding paths.

shown in Scheme 4 which is modified for MO calculations a little. In this scheme, *n*-BuOH (MeOH in Scheme 4) is first treated with EtMgBr to form a Mg²⁺ complex **15** with a *n*-BuO (MeO) ligand. A reaction of **15** with allyl alcohol **3** produces another Mg complex **16**. In this case, nitrile oxide **2** is generated by treatment of **1** with Et₃N. This method worked well and gave high yield as well as regioselectivity like Type III reaction.

After formation of **16**, two possible routes producing **5** are considered. One is that via **18** which has allylic alcohol **3** as a reactant. In the other route, the Mg complex **16** transfers a proton from the alcohol to the alkoxide ligand to form **17**. The intermediate replaces an ether ligand with R¹CNO to form **20**.

The energy-diagram for Scheme 4 (Fig. 3) shows that **17a** (R¹=R²=R³=H) was calculated to be more stable by 1.1 kcal mol⁻¹ than **16a**. The activation energy for the proton transfer from **16a** to **17a** was calculated to be 5.1 kcal mol⁻¹ which is smaller by 4.5 kcal mol⁻¹ than energy difference between **16a** and **18a**. Similarly, **20a** is more stable by 1.3 kcal mol⁻¹ than **18a**. The barrier height for the proton transfer in **18a** is also low, as low as 4.7 kcal mol⁻¹ which is smaller by 11.1 kcal mol⁻¹ than that for **18a(TS)**. Therefore, the proton transfer probably occurs at the beginning of the reaction. As **20a(TS)** is more stable by 4.2 kcal mol⁻¹ than **18a(TS)**, the activation barrier of **20a** with the alkoxide ligand is lower by 2.9 kcal mol⁻¹ than that of **18a** with the alcohol ligand. It is, therefore, considered that **20a** is the reactant for the cycloaddition in the Scheme 4.

Fig. 4 displays the energy profile and the geometry

transformation along the IRC for **20a(TS)**. The energy rises gradually until the TS and decreases gradually until 8.15 amu^{1/2} Bohr. The O(1)–N(2)–C(3) fragment aligns almost straight ((O(1)–N(2)–C(3): 177.4°) until *s* = -4.80 amu^{1/2} Bohr. After this point, the fragment becomes bent gradually in order to change its geometry suitable for cyclization. At the TS (*s* = 0.00 amu^{1/2} Bohr), the O(1)–C(5) length is 2.716 Å longer by 0.594 Å than the C(3)–C(4) length. The (3)–C(4) length at *s* = 4.80 amu^{1/2} Bohr is 1.535 Å which is different by only 0.032 Å from that of the product (1.503 Å) while the O(1)–C(5) is still long (2.108 Å). As the O(1)–C(5) is 1.500 Å in length at *s* = 8.15 amu^{1/2} Bohr, a five membered ring has already formed.

The relation of reactant and TS geometries with the reactivity

The Mg–O(1) lengths in Table 2 are almost the same, ca. 2.1 Å, in all the reactant Mg²⁺ complexes. The Mg–O(7) lengths in the alkoxide complexes (**13a**, **20a**) are shorter than those in the alcohol complexes (**10a**, **18a**). That is, the Mg²⁺ ion binds the alkoxide oxygen atom stronger than the alcohol oxygen. The TSs keep their original features of the geometry in the reactants.

While differences of the C(3)–C(4) lengths in the all TS geometries are less than by 0.043 Å (2.103–2.156 Å), the O(1)–C(5) lengths are closely dependent on the types of reactions. The lengths are in range between 2.710 and 2.716 Å for Type III TSs, between 2.393 and 2.402 Å for Type II TSs, 2.286 Å for Type I TSs. These lengths relate to the activation energies in Table 1. If the present reactions obey the Hammond postulate,¹⁵ in which a TS with a low

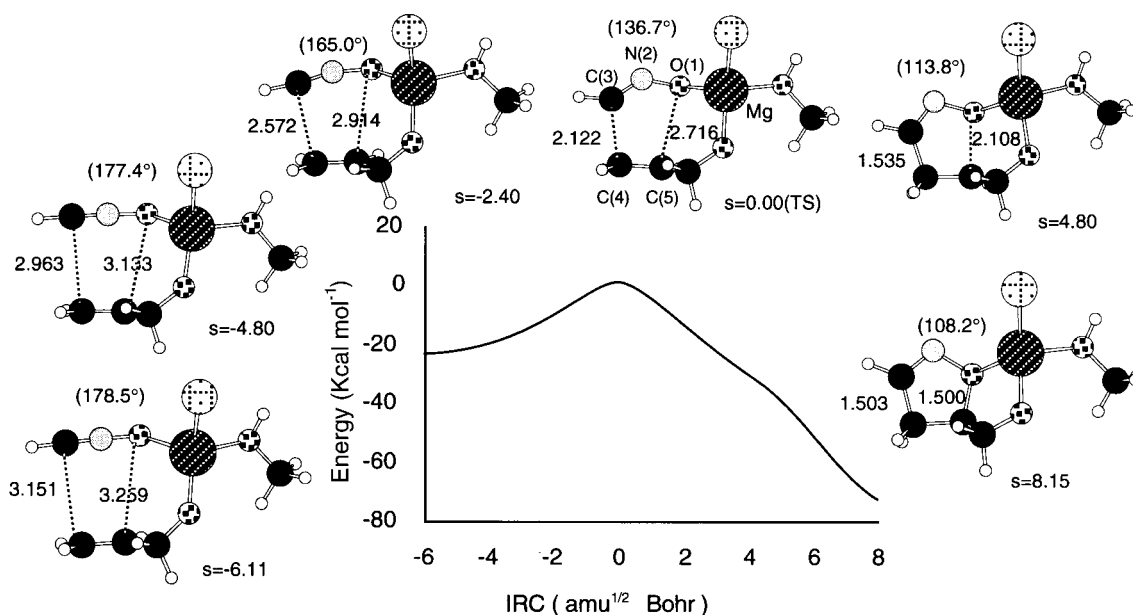


Figure 4. Potential energy profiles and geometry transformation along the IRC of NOC reaction of **20a**. The values in structures are the lengths of O(1)–C(5) or C(3)–C(4) (Å). The values in parentheses are the angle of O(1)–N(2)–C(3) (°).

activation energy locates an early position on reaction coordinate, these lengths closely relate to the activity of Mg complexes. The O(1)–C(5) lengths of Type III reaction is longer and the activation energies are lower than those of Type II reaction.

Stereoselectivity

In the case of allylic alcohol with an alkyl group at the α -position, the magnesium coordination methodology makes it possible to achieve stereoselective cycloadditions. For example, Type I reaction of **2e** ($R^1 = \text{Ph}$) and **3** ($R^2 = \text{Et}$, $R^3, R^4 = \text{H}$) in CH_2Cl_2 gave *syn-5/anti-5* ratio=67:33 while those of Type II and III reactions are 95:5 and 99:1, respectively.^{7b} We examined this propensity using model complex **10**. Fig. 5 displays optimized structures of two isomers, **10b** and **10c**, having a branched methyl group at the α -carbon C(6).

A reactant Mg complex **10b** is an intermediate leading to formation of the *syn*-product and **10c** to the *anti*-product.

The Mg–O(1) and Mg–O(7) length of **10b** (2.048 Å) and **10c** (2.060 Å) are similar to those of **10a** (2.051 Å). As mentioned above, the Mg–O(7) distance is a dominant factor for governing reactivity of intermediates while the methyl group cause no significant change in the lengths. This result suggests that **10b** and **10c** have activation barriers similar to **10a**. Indeed, the activation energies for the cycloaddition of **10b** and **10c** were calculated to be 36.3 and 36.0 kcal mol⁻¹, respectively, at the RHF/6-31G* level of theory (Table 1).¹⁶ These activation energies are almost the same as that of **10a** (36.1 kcal mol⁻¹) without the methyl group at the same level of theory. As the methyl substituent does not change the reactivity at all, the activation energies are not responsible for the stereoselectivity observed in the experiments.

While a small hydrogen H(11) of **10b** is placed at the position *s-cis* to the vinyl group, the methyl group occupies the corresponding position in **10c**. Therefore, $\angle\text{C}(5)\text{--C}(6)\text{--C}(10)$ and $\angle\text{C}(4)\text{--C}(5)\text{--C}(6)$ angles in **10c** (116.6 and 126.2°) are larger by 6.6 and 2.3° than the corresponding

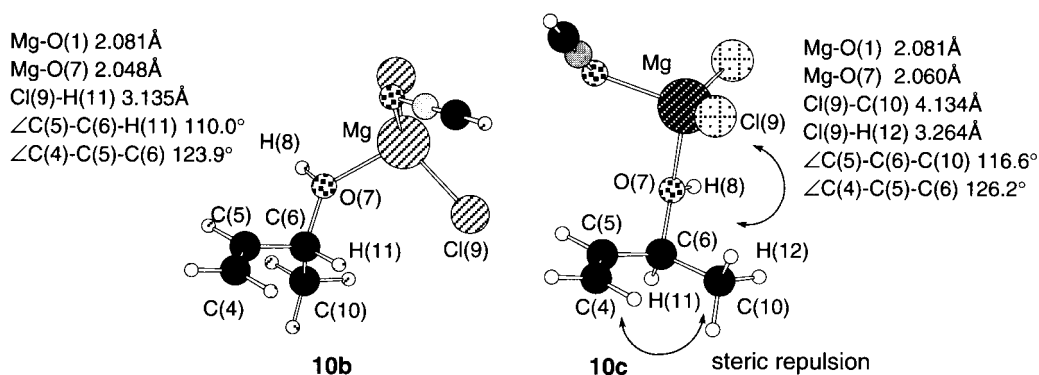


Figure 5. Optimized structures of **10b** and **10c**. The values in the figure are lengths and angles related to the relative stability between the isomers.

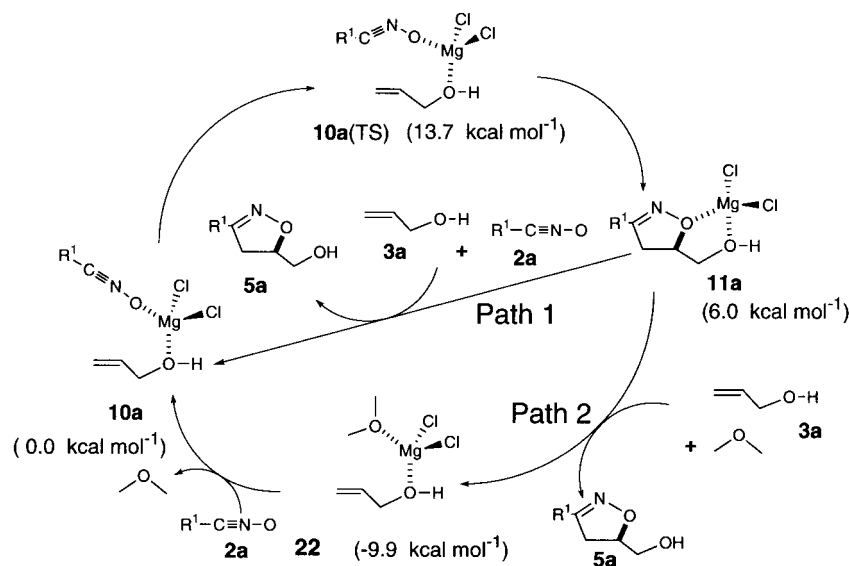


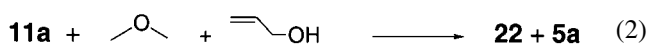
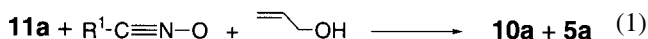
Figure 6. Catalytic cycle of Type II reaction. Values in parentheses are the relative energies at **10a** at MP4(SDTQ)/6-31G**/RHF/6-31G* level of theory.

angles in **10b**. These steric repulsions between the two groups cause **10c** to destabilize by $2.4 \text{ kcal mol}^{-1}$ in comparison with **10b**. The TS structures also inherit this feature in geometry and the relative stability between the intermediates. At the RHF/6-31G* level of theory, **10b(TS)** is more stable by $2.1 \text{ kcal mol}^{-1}$ than **10c(TS)**. A similar result was obtained for the complexes with the alkoxide ligand, **13b** and **13c**. It is, therefore, concluded that the relative stability of the intermediate Mg^{2+} complexes and the TSs is the origin of formation **11** with the stereoselective product, *syn*-**5**. We have already pointed out this relation in a previous paper without calculating the activation energies.^{7b}

Catalytic cycle of magnesium controlled NOC

In Type II reaction, the product Mg complex **11a** is formed through **10a(TS)** from the reactant **10a**, followed by its dissociation. Coordination of **2a** and **3a** to the free MgCl_2 will reproduce **10a**. Therefore, we can expect that catalytic amounts of MgCl_2 are enough to complete a cycle of the catalytic reaction. In fact, catalytic efficiency was reported for $\text{MgBr}_2\text{-Et}_2\text{O}$ in 1,3-dipolar cycloaddition of mesitronitrile oxide to allylic alcohol.¹⁷ Fig. 6 depicts two plausible catalytic cycles for Type II reaction.

It is possible to consider two routes regenerating **10a** in the catalytic cycle. In order to consider energy relation in the catalytic cycle, we have to calculate isodesmic energies of Eqs. (1)–(3).



In Path 1, a bidentate ligand of **11a** is replaced with nitrile oxide and allylic alcohol simultaneously to form **10a**. As the isodesmic energy of the reaction (Eq. 1) turned out to be $6.0 \text{ kcal mol}^{-1}$, Path 1 is an exothermic process. Path 2 is a route passing through the Mg-OMe_2 complex **22**, an alternative intermediate of the catalytic cycle. The product **5a** is replaced with Me_2O and allylic alcohol of **22**. The isodesmic energy of the reaction (Eq. 2) was calculated to be $15.9 \text{ kcal mol}^{-1}$. As a result, replacement of Me_2O with HCNO, which is a necessary step to regenerate the intermediate **10**, is endothermic by $9.9 \text{ kcal mol}^{-1}$.

According to the energy relation of the compounds in Fig. 6, Path 1 is expected to proceed only in the absence of Me_2O since Path 2 is more favorable in energy than Path 1. Path 2 proceeds in the presence of excess amount of Me_2O . These results indicate that THF or Et_2O in the reaction system prevents R^1CNO from binding with the Mg^{2+} in Type II reactions, i.e. decelerating the NOC reactions. It was observed that the large amount of THF actually reduced both the reactivity and selectivity in practice, and the present calculation results is consistent with the experimental results.^{7b}

Concluding Remarks

The formation of the Mg complex is the key for the NOC reactions with high regio- and stereoselectivity. The results obtained in the present work well explain the important role of the Mg^{2+} ion for the 1,3-dipolar cycloadditions of nitrile oxide with allylic alcohol. The following is a summary of our present theoretical study:

1. The Mg control technique is much better than the hydrogen bond strategy because Mg^{2+} can gather oxygen atoms of nitrile oxide and allylic alkoxide strongly and effectively. This geometry of the Mg^{2+} is suitable for the regio- and stereoselectivity observed. It was confirmed that allylic alkoxide instead of allylic alcohol should be

used for experiments in order to obtain complete regioselectivity.

- The LU gaps in the Mg^{2+} complexes are smaller than that in the separated molecules. The order of the energy gap for the three types of reactions are Type III \ll Type II, Type I.
- The Mg–O length (O for alcohol or alkoxide) is closely related to the reactivity of the two ligands in the complexes. The short Mg–O bond in the alkoxide complex results in the activation energy lower than that in the alcohol complex.
- The repulsion between the vinyl fragment and the substituent at the α -position of allylic alcohol or alkoxide determines the stability of the reactant complexes and the TSs. This factor governs the *syn*–*anti* stereoselectivity observed.

Acknowledgements

The authors thank Computer Center, Institute for Molecular Science at the Okazaki National Research Institutes for the use of the NEC HSP computer and Library Program Gaussian94. This study was supported in part by the Grant-In-Aid (Molecular Physical Chemistry, no. 11166249) from the Ministry of Education, Sports and Culture. SF thanks Ube Industries Ltd for the use of Origin computer including Gaussian94 program. The authors also thank Mr Yasuhiro Nagoshi in Information System Group, Corporate Planning and Administration Department at Ube Industries Ltd for technical assistance for calculations.

References

- (a) Jäger, V.; Grund, H.; Buß, V.; Schwab, W.; Müller, I. *Bull. Chem. Soc. Belg.* **1983**, *92*, 1039. (b) Caramella, P.; Grünanger, P. *1,3-Dipolar Cycloaddition Chemistry*; Padwa, A., Ed.; Wiley: New York, 1984; Vol. 1, pp 291–392. (c) Kozikowski, A. P. *Acc. Chem. Res.* **1984**, *17*, 410. (d) Jäger, V.; Grund, H.; Franz, R.; Ehrler, R. *Lect. Heterocycl. Chem.* **1985**, *8*, 79. (e) Curran, D. P. *Advance in Cycloaddition Chemistry*; Curran, D. P., Ed.; JAI Press Inc: Greenwich, Connecticut, 1988; Vol. 1, pp 129–189. (f) Torsell, K. B. G. *Nitrile Oxides, Nitronone, and Nitronate in Organic Synthesis*; VCH: Weinheim, 1988. (g) Annunziata, R.; Cinquini, M.; Cozzi, F.; Raimondi, L. *Gazz. Chim. Ital.* **1989**, *119*, 253. (h) Padwa, A.; Schoffstall, A. M. *Advance in Cycloaddition Chemistry*; Curran, D. P., Ed.; JAI Press Inc: Greenwich, Connecticut, 1990; Vol. 2, pp 1–89. (i) Kanemasa, S.; Tsuge, O. *Heterocycles* **1990**, *30*, 719. (j) Kamimura, A. *J. Synth. Org. Chem. Jpn* **1992**, *50*, 808.
- Recent review on asymmetric 1,3-dipolar cycloaddition: Gothelf, K. V.; Jørgensen, K. A. *Chem. Rev.* **1998**, *98*, 863.
- Huisgen, R.; Christl, M. *Chem. Ber.* **1973**, *106*, 3291 (see also p 3345).
- Recent study on the regiochemistry of the NOC reaction: Caramella, P.; Reami, D.; Falzoni, M.; Quadrelli, P. *Tetrahedron* **1999**, *55*, 7027.
- (a) Martin, S. F.; Dupre, B. *Tetrahedron Lett.* **1983**, *24*, 1337. (b) Müller, I.; Jäger, V. *Tetrahedron Lett.* **1982**, *23*, 4777. (c) Jäger, V.; Schohe, *Tetrahedron* **1984**, *40*, 2199. (d) Jäger, V.; Müller, I. *Tetrahedron* **1985**, *41*, 3519. (e) Kanemasa, S.; Hayashi, T.; Yamamoto, H.; Wada, E.; Sakurai, T. *Bull. Chem. Soc. Jpn* **1991**, *64*, 3274. (f) Caramella, P.; Cellerino, G. *Tetrahedron Lett.* **1974**, *25*, 229. (g) Curran, D. P.; Choi, S. M.; Gothe, S. A.; Lin, F. J. *Org. Chem.* **1990**, *55*, 3710.
- Houk, K. N.; Moses, S. R.; Wu, Y. D.; Ronda, N. G.; Jäger, V.; Schohe, R.; Fronczek, F. R. *J. Am. Chem. Soc.* **1984**, *106*, 3880.
- (a) Kanemasa, S.; Nishiuchi, M.; Wada, E. *Tetrahedron Lett.* **1992**, *33*, 1357. (b) Kanemasa, S.; Nishiuchi, M.; Kamimura, A.; Hori, K. *J. Am. Chem. Soc.* **1994**, *116*, 2324.
- Frisch, M. J.; Trucks, G. W.; Schlegel, H. B.; Gill, P. M. W.; Johnson, B. G.; Robb, M. A.; Cheeseman, J. R.; Keith, T. A.; Petersson, G. A.; Montgomery, J. A.; Raghavachari, K.; Al-Lantham, M. A.; Zakrzewski, V. G.; Ortiz, J. V.; Foresman, J. B.; Cioslowski, J.; Stefanov, B. B.; Nanayakara, A.; Challacombe, M.; Peng, C. Y.; Ayala, P. Y.; Chen, W.; Wong, M. W.; Andrés, J. L.; Replogle, E. S.; Gomperts, R.; Martin, R. L.; Fox, D. J.; Binkley, J. S.; Defrees, D. J.; Baker, J.; Stewart, J. J. P.; Head-Gordon, M.; Gonzaléz, C.; Pople, J. A. *Gaussian94*; Gaussian, Inc.: Pittsburgh, PA, 1995.
- Win MOPAC, version 2; Fujitsu, 1998.
- (a) Fukui, K. *Acc. Chem. Res.* **1981**, *14*, 363. (b) Head-Gordon, M.; Pople, J. A. *J. Chem. Phys.* **1988**, *89*, 5777.
- (a) Fukui, K. *Acc. Chem. Res.* **1971**, *4*, 57. (b) Fleming, I. *Frontier Orbitals and Organic Chemical Reactions*; Wiley-Interscience: New York, 1976.
- Sustmann, R. *Tetrahedron Lett.* **1971**, *12*, 2717.
- MOs in Fig. 1 are not the real HO or LUMOs, which are not, in common, related to the 1,3-cycloaddition in complexes. We regarded the MOs in the figure as FMOs in the reaction.
- The value is almost same as that ($4.9 \text{ kcal mol}^{-1}$) from the RHF/3-21G level of theory as described in Ref. 6.
- (a) Hammond, G. S. *J. Am. Chem. Soc.* **1955**, *77*, 334. (b) Streitwieser, Jr. A. *Chem. Rev.* **1956**, *56*, 639.
- We used the energies at the RHF/6-31G* level of theory in this section because of lack of computer facility calculating the MP4(SDTQ) energies of **10b** and **10c** with an additional α -methyl substituent.
- Kanemasa, S.; Okuda, K.; Yamamoto, H.; Kaga, S. *Tetrahedron Lett.* **1997**, *38*, 4095.